Charge-exchange, ionization and excitation in low-energy Li^+- Ar, K^+- Ar, and Na^+-He collisions.

Ramaz A. Lomsadze[1], Malkhaz R. Gochitashvili[1], RomanYa. Kezerashvili[2,3],* and Michael Schulz[4]
[1] *Tbilisi State University, Tbilisi, 0128, Georgia*
[2] *Physics Department, New York City College of Technology, The City University of New York, Brooklyn, NY 11201, USA*
[3] *The Graduate School and University Center, The City University of New York, New York, NY 10016, USA and*
[4] *Missouri University of Science and Technology, Rolla, MO 65409, USA*
(Dated: July 4, 2016)

Absolute cross sections are measured for charge-exchange, ionization, and excitation within the same experimental setup for the Li^+-Ar, K^+- Ar, and Na^+- He collisions in the ion energy range $0.5-10$ keV. Results of our measurements along with existing experimental data and the schematic correlation diagrams are used to analyze and determine the mechanisms for these processes. The experimental results show that the charge-exchange processes are realized with high probabilities and electrons are predominately captured in ground states. The cross section ratio for charge exchange, ionization and excitation processes roughly attains the value $10:2:1$, respectively. The contributions of various partial inelastic channels to the total ionization cross sections are estimated and a primary mechanism for the process is defined. The energy-loss spectrum, in addition, is applied to estimate the relative contribution of different inelastic channels and to determine the mechanisms for the ionization and for some excitation processes of Ar resonance lines for the K^+-Ar collision system. The excitation function for the helium, as well as for the sodium doublet lines for the Na^+-He collision system, reveals some unexpected features and a mechanism to explain this observation is suggested.

PACS numbers: 34.80.Dp, 34.70.+e, 34.50.Fa, 32.80.Zb

arXiv:1607.00296v1 [physics.atom-ph] 1 Jul 2016

I. INTRODUCTION

The exploration of inelastic processes, with the goal of obtaining reliable data on the corresponding cross section, are considered as a powerful tool in understanding the dynamics taking place in slow ion−atom collisions. Usually, models using a molecular basis set are applied to determine the transition probabilities between the terms corresponding to the main inelastic channels. However, such terms, due to the complicated many-channel character, have been calculated for only a small number of simple collision systems. Therefore, the schematic correlation diagrams of diabatic molecular orbitals are widely used. However, they provide only a qualitative explanation of the processes. The situation becomes more problematic from an experimental point of view when particles with closed electron shells are involved in the collision process. There are several reasons for this, but mainly it is related to the following: 1) precise measurements of cross sections for ionization and charge exchange processes require collection and identification of all secondary particles; 2) a reliable determination and control of the relative and absolute spectral sensitivity of the light-recording system while performing an optical measurement is needed. It is known that in such collisions these processes take place at relatively small impact parameters corresponding, on avarage, to large momentum transfers. Because of this the inelastic processes are realized when the incident ions are scattered through relatively large angles and, due to momentum conservation, this is accompanied by the formation of much more energetic secondary particles than for weakly bound valence electrons. The energy of these secondary particles (ions and free electrons) may reach tens of electron volts, therefore, their full collection is problematic. At the same time, these secondary particles along with primary particles are used to determine cross sections. This circumstance has not been considered in the earlier works [1–4] measuring cross sections for ionization and charge-exchange processes. Therefore, some doubts related to the reliability of these data and, hence, conclusion drawn from them, seem to be indicated. For example, in case of ionization processes, a standard capacitor method was used [1] which yields significant inaccuracies in measurements of cross sections, because no measures were taken to prevent the scattering of primary and high-energy secondary ions. As to charge-exchange processes, the magnitude of almost all previously obtained cross sections [1, 2, 4] are underestimated, which is caused by the fact, that the method used for the detection of neutral particles failed to ensure collection of those particles which were scattered through large angles. Therefore, it is necessary

*Electronic address: rkezerashvili@citytech.cuny.edu

to reinvestigate some collision systems more accurately and some for the first time. These studies require combined experimental approaches, incorporating with the methods which are free of the deficiencies mentioned above, and a variety of reliable experimental data for more persuasive interpretation. From the other side one can use schematic correlation diagrams to interpret the data and to identify the mechanisms leading to the processes being investigated. Research on alkali-metal ion collisions with rare gas atoms have been carried out by a variety of methods [1–23], however the available data for the absolute cross sections of the above mentioned processes are not always consistent with each other [1, 3, 4, 10, 13] and in some cases, unreliable [2].

The objectives of present work are detailed studies of processes induced by an interaction of closed-shell alkali-metal ions of Li^+, K^+, and Na^+ with atoms of rare gases Ar and He. We performed measurements of absolute differential and total cross sections for charge-exchange, ionization and excitation processes in Li^+-Ar, K^+-Ar, and Na^+-He collisions in the range of ions energy 0.5−10 keV. In collisions of a Li^+, K^+, or Na^+ ion beam with Ar and He atoms we focus on the following charge-exchange processes:

$$Li^+ + Ar \rightarrow Li + Ar^+, \quad (1)$$
$$K^+ + Ar \rightarrow K + Ar^+, \quad (2)$$
$$Na^+ + He \rightarrow Na + He^+, \quad (3)$$

where the products of the reaction can be in the ground states or in different excited states. The collisions can induce the following ionization processes:

$$Li^+ + Ar \rightarrow Li^+ + Ar^+ + e, \quad (4)$$
$$K^+ + Ar \rightarrow K^+ + Ar^+ + e, \quad (5)$$
$$Na^+ + He \rightarrow Na^+ + He^+ + e. \quad (6)$$

The reactions (4) - (6) represent ionization processes for the target atoms, that include different channels for the excitation of the produced ions of the target atoms or/and incident ions, as well as the excitation of autoionization states of the target atom that leads to its ionization. In collisions of K^+ and Na^+ ions with Ar and He atoms our study is focused on the following excitation processes:

$$K^+ + Ar \rightarrow K^{+\,*} + Ar^*, \quad (7)$$
$$Na^+ + He \rightarrow Na^{+\,*} + He^*. \quad (8)$$

The excitation processes (7) and (8) include different channels for excitation of the K^+ or/and Ar atom, and the Na^+ ion or/and He atom, respectively.

Charge-exchange cross sections for the K^+-He, K^+-Ne, K^+-Ar, K^+-Kr, K^+-Xe collision systems were reported in Ref. [2] using the detection of fast neutral particles with a restricted interval of scattering angles. However, as shown in Ref. [12], this limiting condition on the interval for collision angles in Ref. [2] underestimated the measured charge-exchange cross sections for all collision systems and, particularly, for K^+- Ar this underestimation reaches more than a factor of ten. The absolute excitation cross section of the potassium resonance spectral line for the K^+-Ar collision is reported in Ref. [27], however it was measured just for low energies, up to 0.7 keV. A convincing result, though in a limited energy interval 1−3 keV, for the excitation cross section of summed spectral Ar lines $\lambda = 104.8 - 106.7$ nm in K^+-Ar collision system are presented in Ref. [26]. Double differential cross sections for the K^+-Ar collision system have also been measured in Ref. [12]. An inelastic collision mechanism for the systems of Li^+-He and Li^+-Ne has been studied experimentally and theoretically in Ref. [8, 9, 18, 24, 25]. An absolute value of the differential cross section at two fixed energies, $E = 200$ eV and $E = 350$ eV of Na^+ ions, is reported in Ref. [11]. A relative differential cross section for the Na^+-Ar collision system is measured in Ref. [17]. The most comprehensive study for excitation mechanisms in Na^+-He and K^+-He collisions, at the ion energies of $1.0 - 1.5$ keV and by the differential spectroscopy, were reported recently in Ref. [23]. Double differential cross sections were measured by detecting all scattering particles (Na^+, Na, K^+, K, He^+, He) over a wide range of scattering angles.

For the Na^+- Ar collision an energy spectrum of electrons ejected from autoionization states of Ar atoms at $E = 15$ keV [15] have been reported, but no result exist for low energy collisions. The result of the measurements for the excitation function for the Na^+-He and K^+-He collision systems, though in arbitrary units are reported in Refs. [5, 6]. A normalized emission cross section of He resonance atomic lines for Na^+-He collisions are presented in Ref. [28]. Another comprehensive study of slow ion-atom collisions with closed electron shells was carried out for the Na^+-Ne [16], although measurements were performed for a limited energy interval.

This brief survey of above mentioned processes occurring in alkali-metal ion impact with atoms of rare gases shows that today there is no systematic experimental measurements and reliable data available. Most of experimental results

are either provided in arbitrary units or reported for a restricted energy interval. To our mind, the reason for this scarcity of measurements is linked with the difficulties of performing the research with close electron shell particles: scattering on large angles and problem of collection of secondary particles. This circumstance motivates the present detailed investigation of the primary mechanisms for these collision processes. We have so far studied collisions between closed electron shell particles for the K^+-He, Na^+-Ne, Na^+-Ar, Ne^+-Na, and Ar^+-Na collision systems [14, 19, 22]. In this paper, we report systematic studies of absolute total cross sections for charge-exchange, ionization and excitation for the Li^+-Ar, K^+-Ar, and Na^+-He collisions in a broad range of collision energies (0.5−10 keV), as well as the energy-loss spectra for the K^+-Ar collision system. We have also measured the energies of the electrons liberated in the collisions. We have found that for the K^+-Ar collision, the energy of most of the liberated electrons are within the interval 20−32 eV, the electrons' energy are less than 17 eV for the Na^+-He collision, and below 12 eV for the Li^+-Ar collision system.

The remainder of this paper is organized as follows: in Sec. II. the experimental techniques and measurement procedures are described and three different experimental methods of measurements are presented. Here we introduce the procedures for measuring of absolute total and differential cross sections for charge-exchange, ionization and excitation processes. The description of our measurements and the comparison of them with the results of previously obtained experimental studies for the charge-exchange, ionization and excitation occurring in the Li^+-Ar, K^+-Ar, and Na^+-He collisions are given in Sec. III. The discussion of experimental results, and determination and clarification of the mechanisms for the charge-exchange, ionization and excitation processes are presented in Sec. IV. Finally, in Sec.V, we summarize our investigations and present the conclusions.

II. EXPERIMENTAL TECHNIQUES AND MEASUREMENT PROCEDURES

2.1. The main experimental set-ups used in the present experiments for measurements of total and differential cross sections for charge-exchange, ionization and excitation processes are the following: i. the refined version of a capacitor method; ii. a collision spectroscopy method; iii. an optical spectroscopy method. The basic approach for measurements of inelastic processes realized in collision of an alkali-metal ion with rare gases atoms was described previously in Ref. [22], so only the details of the apparatus with description outline of methods and measurement procedures will be given here. A beam of Li^+ , K^+, or Na^+ ions from a surface-ionization ion source is accelerated, formed, and focused by an ion-optics system, which includes quadruple lenses and collimation slits [22]. After the beam passes through a magnetic mass spectrometer, it enters the collision chamber containing target Ar or He gasses. The pressure in the collision chamber is kept at about 10^{-6} Torr, while the typical pressure under operation with the Ar and He target gasses is a two order of magnitude less. This ensures single-collision conditions for the ion-target atom collision. The charge-exchange and ionization cross section were measured by a refined version of the capacitor method [29]. This method allows preventing the electrodes by the scattering primary ions that affect the results of measurement. The secondary positive ions and free electrons produced during the collision are collected and detected by a collector. The collector consists of two rows of plate electrodes that ran parallel to the primary ion beam. A uniform transverse electric field, that extracts and collects secondary particles, is created by the potential applied to the grids. This method represents a direct measurement of the yield of produced singly positively charged ions and free electrons as the primary beam passes through the target gas. Obviously, the measured quantities are related to the capture cross section and the apparent ionization cross section [22]. The uncertainties in the measurements of the charge-exchange cross sections for the Li^+-Ar, K^+-Ar, and Na^+- He collision systems are estimated to be 7%, 15%, and 10%, respectively, while the uncertainties in the measurements of the ionization cross sections are estimated to be 12%, 10%, and 15%, respectively. These uncertainties are determined primarily by the uncertainties in the measurements of absolute value of the cross sections for production of positively charged ions and free electrons, as the primary beam passes through the target, and by the uncertainty in the measurement of the target gas pressure in the collision chamber.

2.2. The energy-loss spectra and differential scattering experiments are performed by the collision spectroscopy method. Since the details of the apparatus have been given elsewhere [30], only a brief description is presented here. The primary beam extracted from the ion source was accelerated to the desired energy before being analyzed according to q/m (q and m are the ion's charge and mass, respectively). The analyzed ion beam after being collimated by a slit enters into the collision chamber and then passes into a "box" type electrostatic analyzer. The energy resolution of this analyzer is $\Delta E/E = 1/500$. The voltage applied to the analyzer is scanned automatically which allows to investigate the energy-loss spectra in the energy range of $0 - 100$ eV. The differential cross section is measured by rotating the analyzer around the center of collision over an angular range between 0^0 and 20^0. The laboratory angle is determined with respect to the primary ion beam axis with an accuracy of 0.2^0. Such a tool gives us the option to determine the total cross sections and compare them with the results obtained by the refined version of the capacitor method [29]. In addition, the measured energy-loss spectra provide detailed information related to the intensity of

inelastic processes realized in the charge-exchange, ionization and excitation reactions.

2.3. The method used for the optical measurements was discussed previously in Ref. [31], therefore, only brief description will be given here. The alkali-metal ion beam leaving the surface-ionization ion source after acceleration to a predetermined energy is focused by the quadruple lenses and analyzed by a mass-spectrometer. The emerging ions passes through a differentially pumped collision chamber with the target gas at low pressure. The light emitted from the collision chamber as a result of the excitation of colliding particles, is viewed perpendicularly to the beam by an optical spectrometer. The spectral analysis of the radiation is performed in the vacuum ultraviolet and in the visible spectral regions. The linear polarization of the emission in the visible part of the spectra is analyzed by a Polaroid and a mica quarter-wave phase plate. A photomultiplier tube with a cooled cathode is used to analyze and detect the emitted light. The spectroscopic analysis of the emission in the vacuum ultraviolet spectral region is performed with the Seya – Namioka vacuum monochromator incorporating a toroidal diffracting grating. The radiation is recorded by the secondary electron multiplier used under integrating or pulse-counting conditions. The polarization of the radiation in the vacuum ultraviolet region is not taken into account. We determine the absolute excitation cross sections by comparing the measured output signal with the one that is obtained due to the excitation of nitrogen molecule by electron impact. Particular attention is, therefore, devoted to the reliable determination and control of the relative and absolute spectral sensitivity of the light-recording system in the visible part of spectra. The latter is done by measuring the photomultiplier output signal due to the bend of the first negative system of the ion N_2^+ ($B^2\Sigma u^+ - X^2\Sigma g^+$ transition) and due to the Mainel system ($A^2\Pi u^+ - X^2\Sigma g^+$ transition) excited in collisions between the electrons and nitrogen molecules [32]. These bands cover the wavelength interval between 423.6 nm and 785.4 nm. The output signal is normalized to the (0.1) band ($\lambda = 427.8$ nm) which has the highest intensity in this range. The relative spectral sensitivity of the light recording system obtained in this way is compared with the measured relative excitation cross sections for the same bands, averaged over the experimental data reported in Refs. [33–38]. The absolute uncertainties in the excitation cross section for the $K^+ - Ar$ and $Na^+ - He$ colliding system are estimated to be 15% and the uncertainty of relative measurements is about 5%.

III. RESULTS OF EXPERIMENTAL MEASUREMENTS

3.1. The measured energy dependences of the absolute cross section for the charge-exchange, ionization and excitation processes are presented in Figs. $1-3$. Figure 4 represents a typical example of the energy-loss spectrum for $K^+ - Ar$ collisions. Figs. $1-3$ reveal marked differences between the energy dependences of the cross sections for the various processes. While the ionization cross section shown in Fig. 2 increases monotonically with energy, the charge-exchange cross section has almost a flat energy dependence, and the excitation function exhibits an oscillatory structure. Another feature is the magnitude of the cross sections. Among of the processes investigated the largest value of cross section has charge-exchange processes. The data for the charge-exchange cross sections for the $Li^+ - Ar$, $K^+ - Ar$, and $Na^+ - He$ collisions with electron capture to the ground state of potassium K($4s$) state for the $K^+ - Ar$, lithium Li($2s$) state for the $Li^+ -$ Ar, and sodium Na($3s$) state for the $Na^+ - He$ collision systems, respectively, are presented in Fig. 1. In the same figure are presented the charge-exchange in the excited resonance K($4p$) state, for the $K^+ - Ar$, and Na($3p$) state, for the $Na^+ - He$. For comparison we also present in Fig. 1 the data of other authors. The comparison of our charge-exchange cross sections for the $K^+ - Ar$ collision sytem (curve 1a) with the results from Ref. [39] at a fixed impact energy $E = 350$ eV (open square) and results obtained in Ref.[12] at a fixed impact energy $E = 2$ keV (open triangle) shows satisfactory agreement within the experimental uncertainties. However, a dramatic difference, by about two orders of magnitude as well as in the shape of the energy dependences are observed when one compares our results for the $K^+ - Ar$ system (curve 1a) with data from Ref. [1] (curve 1b). The same tendency, but with a smaller discrepancy of one order of magnitude, is observed when one compares our results for the $Li^+ - Ar$ (curve 2a) and $Na^+ - He$ with the results from Ref. [2] (curves 2b and 3b, respectively). Our results for the $Na^+ - He$ charge-exchange processes (curve 3a) can be compared with the cross section obtained in differential scattering experiments [17] at energy of $E = 1.5$ keV, (open circle). This comparison shows that here the discrepancy only amounts to a factor of three. At and below 1.5 keV impact energy our excitation cross section for K($4p$) state in the $K^+ -$ Ar collision (curve 1c) in energy region $E < 1.5$ keV is in satisfactory agreement with the earlier data [27] (curve 1d).

3.2. The data for the ionization cross section for the $Li^+ - Ar$, $K^+ - Ar$, and $Na^+ - He$ collisions, along with the previously obtained measurements, are shown in Fig. 2. Here curve 1a represents ionization cross section for the $K^+ - Ar$, curve 2a – for the $Li^+ - Ar$ and curve 3a – for the $Na^+ - He$ collision systems. The comparison of our ionization cross section for the $K^+ - Ar$ collision (curve 1a) with the results obtained in Ref. [1] (curve 1b) and the results obtained at a fixed $E = 2$ keV impact energy in Ref. [7] (open triangle), as well as comparison of our results for the $Li^+ - Ar$ collision system (curve 2a) with the results from Ref. [1] (curve 2b) shows a satisfactory agreement in the energy range studied. Satisfactory agreement are observed also at low energies while comparing our results

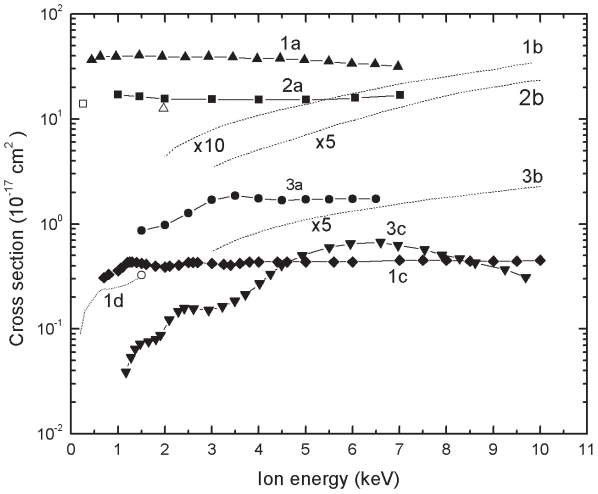

FIG. 1: Dependences of the absolute charge-exchange cross sections on energy of Li^+, K^+ and Na^+ ions in Li^+-Ar , K^+-Ar, and Na^+-He collisions. Results of the present study in comparison with the previous measurements from Refs. [1, 2, 12, 23, 27, 39]. Curves: 1a − electron capture in the ground potassium K($4s$) state for the K^+- Ar system, present data; 1b − electron capture in ground potassium K($4s$) state for the K^+-Ar, data from Ref. [1] are multiplied by a factor of 10; 1c − electron capture in the excited resonance K($4p$) state ($\lambda = 766.5 - 769.8$ nm, transition $4p - 4s$) for the K^+-Ar collision, present data ; 1d − electron capture in excited resonance K($4p$) state ($\lambda = 766.5$ nm, transition $4p - 4s$) for the K^+-Ar, data from Ref. [27]; □ − electron capture in the ground potassium K($4s$) state, for the K^+-Ar system, data from Ref. [39]; △ − electron capture in the ground potassium K($4s$) state for the K^+-Ar, data from Ref. [12]; 2a − electron capture in ground lithium Li($2s$) state for the Li^+-Ar system, present data; 2b − electron capture in ground lithium Li($2s$) state for the Li^+-Ar sytem, data from Ref. [2] are multiplied by a factor of 5; 3a − electron capture in ground sodium Na($3s$) state for the Na^+-He system, present data; 3b − electron capture in ground sodium Na($3s$) state for the Na^+-He, data from Ref. [2] are multiplied by a factor of 5; ◯ − electron capture in ground sodium Na($3s$) state for the Na^+-He system, data from Ref. [23]; 3c − electron capture in excited resonance sodium Na ($3p$) state ($\lambda = 589.0 - 589.6$ nm, transition $3p - 3s$) for the Na^+-He, present data.

for the Na^+-He (curve 3a) with the result from Ref. [1] (curve 3b), but the discrepancy increases for ion energies $E > 5$ keV. A rather significant discrepancy is observed if one compares our results for K^+-Ar (curve 1a) with the previously obtained results in Ref. [4] (curve 1c). Our experimental results for the ionization cross section for the Li^+-Ar collision system (curve 2a) are in an excellent agreement with theoretical prediction [40] (curve 2c).

3.3. The results of measured excitation cross sections realized for the K^+-Ar and Na^+-He collisions, along with the data obtained by other authors, are presented in Fig. 3. The data obtained in our study for the excitation function of the argon atomic resonance line ($\lambda = 106.7$ nm, $3p^5 4s - 3p^6$ transition) emitted in the K^+-Ar collision are presented by curve 1a. The excitation cross section for the resonance spectral Na doublet lines, $\lambda = 589.0$ nm and $\lambda = 589.6$ nm, $3p - 3s$ transition, in the Na^+-He collision is presented by curve 3a, while the resonance helium atomic line, $\lambda = 58.4$ nm, $2p - 1s$ transition, and the sum of the excitation cross section of sodium and helium lines in collisions between sodium ions and helium atoms, are presented by curves 3a, 2a, and 4a, respectively.

Comparison of our data for the excitation function for the sodium doublet and for the helium atom with the results reported in Refs. [28, 41] shows, that there is a considerable discrepancy in magnitude of the excitation cross sections. Moreover, significant discrepancies are observed also in the energy dependence of the excitation cross section for the sodium doublet with the exception of the position of the maximum at $E = 6.5$ keV. Our observations show an oscillating structure of the cross section which was not seen in Ref. [41]. Our results for the energy dependence with a pronounced oscillatory structure on the excitation cross section of the helium atom are the same as in Ref. [18] and the oscillations are in phase, but there are discrepancies in the magnitude. The discrepancies, as compared with Ref. [41], are due to the considerable experimental uncertainties introduced by the photographic method employed in Ref. [41] to record the radiation. This is also the explanation of the discrepancy between the magnitudes of our results and the results obtained in Ref. [41], (curve 3b) since the data from Ref. [41] were used in Ref. [28] to determine the absolute value of these cross sections. The comparison of our results for the excitation of the Ar resonance $4s$, line $\lambda = 106.7$ nm (curve 1a) with the results from Ref. [26], (curve 1b) is difficult because the data in Ref. [26] are obtained in the limited energy interval from 1 to 3 keV and they considered excitation of the Ar resonance $4s$ as the sum of lines $\lambda = 104.8$ nm and $\lambda = 106.7$ nm. The difference between our results of the helium atomic resonance line

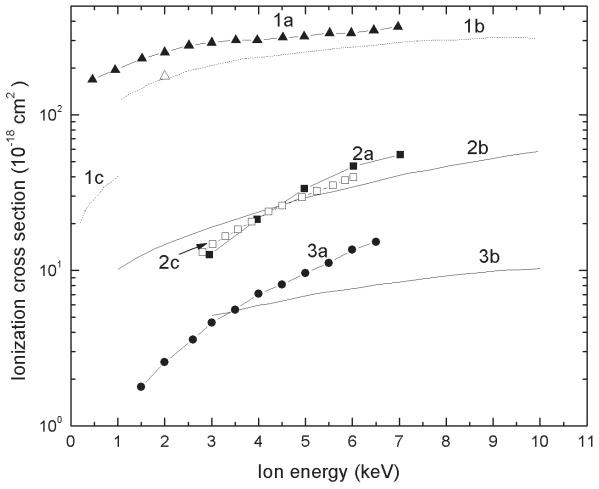

FIG. 2: Dependences of the absolute ionization cross sections on energy of Li^+, K^+, and Na^+ ions in the Li^+-Ar, K^+-Ar, and Na^+-He collisions. Results of the present study in comparison with the previous measurements from Refs. [1, 4, 7, 40]. Curves: 1a – K^+-Ar, present data; 1b - K^+-Ar, data from Ref. [1]; 1c- K^+-Ar, data from Ref. [4]; △- K^+-Ar, data from Ref. [7]; 2a – Li^+-Ar, present data; 2b – Li^+-Ar, data from Ref.[1]; 2c- Li^+-Ar, data from Ref. [40]; 3a – Na^+-He, present data; 3b - Na^+-He, data from Ref. [1].

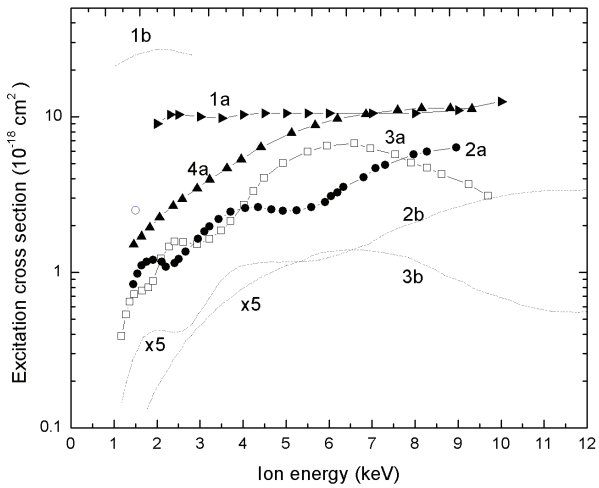

FIG. 3: Excitation cross sections for the resonance argon atomic line for the K^+-Ar collision system, and for the resonance lines of sodium doublet and helium atom in the Na^+-He collision. Results of the present study in comparison with the previous measurements from Refs. [23, 26, 28, 41]. Curves: 1a - excitation function of the resonance argon atomic line $\lambda = 106.7$ nm , $3p^5 4s - 3p^6$ corresponding to the transition $3p^5 4s - 3p^6$ in the K^+-Ar collision system, present data; 1b - excitation function of the summed resonance argon atomic lines $\lambda = 104.8$ nm and 106.7 nm corresponding to the transions $3p^5 4s - 3p^6$ and $3p^5 4s' - 3p^6$ for the K^+-Ar collision sytem, data from Ref. [26]; 2a, 2b and ◯- excitation function of the resonance helium atomic line $\lambda = 58.4$ nm corresponding to the $2p - 1s$ transition in the Na^+-He collision system, present data, data from Ref. [28] multiplied by a factor of 5 and data from Ref. [23], respectively; 3a and 3b - excitation function of the resonance sodium doublet lines $\lambda = 589.0$ nm and 589.6 nm for the transition $3p - 3s$ in the Na^+-He system, present data and data from Ref. [41] multiplied by a factor 5, respectively; 4a – the summed excitation cross sections of the resonance helium atomic line (curve 2a) and resonance sodium doublet lines (curve 2b), for the Na^+-He collision, present data.

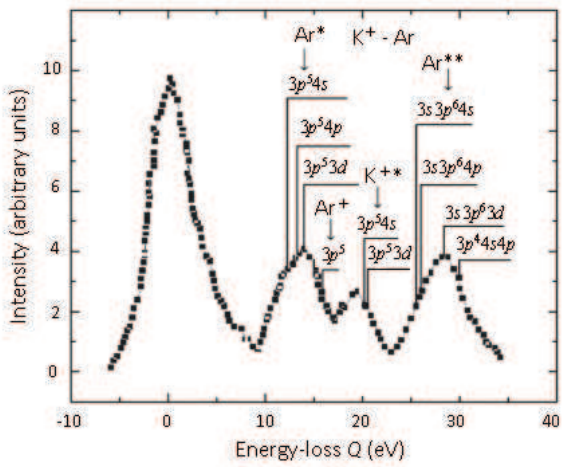

FIG. 4: Typical energy-loss spectrum in laboratory reference system for K^+-Ar collisions measured at $E = 2$ keV collision energy and $\theta = 3.5^0$ scattering angle.

(curve 2a) and those from Ref. [23] obtained at fixed energy, $E = 1.5$ keV (open circle) reaches threefold.

3.4. We studied the energy-loss spectrum for the K^+-Ar collision system and a typical example of the inelastic energy-loss spectrum for K^+-Ar collisions is presented in Fig. 4. The same spectrum was presented in our previous paper [22] for reference. In the present study this spectrum will be used to investigate which mechanism is dominant in the K^+-Ar collisions. Generally, in our study for this collision system, we measured spectra through different fixed angles in the range $1^0 - 7^0$. However, the spectrum in Fig. 4 is chosen for a fixed energy of $E = 2$ keV and scattering angle $\theta = 3.5^0$ at which the inelastic channels are well pronounced. It is seen from figure that the spectrum has a discrete character. The first peak of this spectrum with zero energy-loss corresponds to the elastically scattered ions. The second peak in the spectrum corresponds to the single electron excitation of the argon atom into $3p^54s$, $3p^54p$ and $3p^53d$ states with the energy-loss Q within $11.6 - 14.0$ eV, and a single ionization of the Ar atom in the state $3p^5$at the energy-loss of 15.7 eV. The third peak correspond to the excitation of K^+ ion into the $4s$ and $3d$ states with the energy-loss $16 < Q < 22$ eV, while the fourth one to the excitation of autoionization states of the Ar atom with the excitation of one $3s$ electron or two $3p$ electrons, and to the ionization with the excitation of the Ar, with the energy-loss of $25 < Q < 32$ eV. An investigation of the dependence of the area of each of the peaks versus the scattering angle of the incident ions has shown that the excitation cross sections of the investigated transitions exhibits an onset behavior. Acritical s the scattering angle is increased, the cross section of each inelastic transition remains small, up to a certain scattering angle θ_c. When θ_c is reached the cross section of the transition increases sharply. With further increase of the scattering angle the cross sections of the inelastic transitions decreases. Such onset behavior of the angular dependences of differential cross sections for the inelastic transitions makes it possible to integrate these cross sections for the estimation of relative contribution of different inelastic channels, and compare them with the obtained total cross section. In our study such approach has been applied to determine the mechanism for the ionization processes and for some excitation processes of Ar atoms realized in the K^+-Ar collision that is presented in Sec. IV.

IV. DISCUSSION OF EXPERIMENTAL RESULTS AND MECHANISMS OF PROCESSES

A. Charge exchange in Li^+-Ar , K^+-Ar, and Na^+-He collision systems

We use the experimental data for the individual inelastic channels along with the corresponding schematic correlation diagrams to establish the mechanism for the charge-exchange processes for the Li^+-Ar, K^+-Ar, and Na^+-He collision systems.

1. Li^+-Ar collisions

The results of the charge-exchange cross sections for the Li^+-Ar collision system are presented in Fig. 1 by curve 2a. It is seen that the dependence of the cross sections on the energy of Li^+ ions is weak. No oscillations are seen in

the cross section, and its average value amounts to $1.4{\cdot}10^{-16}$ cm^2.

The inelastic differential cross section measurements for the Li^+ ion collisions with rare gases have been performed in the keV energy range in Ref. [42]. Besides, in that work using a single electron configuration approximation, the calculations are reported for the potential curves of Σ symmetry, corresponding to the ground state of the system and to the one and two electron excitation states of colliding particles. From these calculations it follows that there are two coupling regions in which non-adiabatic transitions may cause charge-exchange: one occurs at internuclear distance $R \sim$1.5 a.u., and the other at $R \leq$0.5 a.u. Also the authors suggested, that in both cases the most probable mechanism responsible for the charge-exchange process is the transition from the ground state of the system to the state corresponding to the electron capture into the ground state of lithium Li($1s^2 2s$) as it is seen from the correlation diagram in Fig 5. The transition for the non-adiabatic region, corresponding to the internuclear distance $R \sim 1.5$ a.u., has been also observed in experiments [42] by measuring differential cross sections. Unfortunately, the transition region at $R \leq 0.5$ a.u. was not investigated in Ref. [42], since the scattering was studied up to 25 keV·deg., which means that the particles approach each other only up to $R \geq 0.75$ a.u. For estimation of the contribution of the transition at $R \leq 0.5$ a.u. to the total charge-exchange cross section, we integrate the differential cross section given in Ref. [42] at energy of $E = 3$ keV and compare with our result. The comparison shows that the results coincide well each other within the experimental uncertainties. Therefore, one can conclude that the contributions from transitions corresponding to $R \leq 0.5$ a.u. to the charge-exchange cross section is negligible and the contribution of the transition at $R \sim 1.5$ a.u. to the charge-exchange cross section is the dominant one. A possible reason for the importance of this region, where the terms of $X^1\Sigma$ and $A^1\Sigma$ energetically approach each other, is the prevalence of the attraction between the Ar^+ ion and Li atom due to polarization over the repulsion caused by the exchange interaction at those distances.

2. K^+-Ar collisions

To determine the mechanism for the K^+-Ar collisions we compare the total charge-exchange cross section presented in Fig. 1 by curve 1a with those corresponding to the decay of resonance levels of the potassium atom, presented by curve 1c. Taking into account the selection rules and the ratio of oscillator strengths for the transitions, we show that the decay of any of the excitation levels of the potassium atom culminates in about half the cases with a transition of the atom to a resonant state, which then decays. Thus, the doubled de-excitation cross section of the potassium atom gives a clue related to the capture cross section in the excited state. The comparison of this two sets of our results show that the contribution to the cross section from capture of an electron to the excited $4p$ state of potassium atom to the total charge-exchange cross section is small, so that the main contribution is provided by the capture to the $4s$ ground state. However, the energy dependence of these cross sections is the same: the cross sections reach their maxima at low K^+ energies $E \sim 1$ keV and vary slowly in a wide energy range. The experimental results for the K^+-Ar collision that leads to the charge-exchange can be explained qualitatively in terms of the schematic correlation diagrams for molecular orbitals given in Ref. [44]. The analysis of this diagram shows that the capture to the ground $4s$ and excited $4p$ states of the potassium atom can occur as a result of a transition between terms of the same $\Sigma - \Sigma$ symmetry. The processes responsible for the population of these states are competing processes. This conclusion is supported by the fact that the terms corresponding to these states are populated from the same initial state term. Moreover, the parameters of the quasi-crossing region are such that the emission maxima occur for equal velocities. Substantial discrepancies between the magnitudes of the cross section are linked to the crossing point R of molecular terms and can probably be explained by the fact that the processes are occurred in different crossing points R of molecular terms. The initial state term at first populates the term corresponding to the ground $4s$ state at large internuclear distance R, and after that to the excited $4p$ state at comparatively smaller distances R. These considerations lead to the conclusion that charge-exchange into the ground $4s$ state and excited $4p$ state of the potassium atom involves the Landau-Zener type interaction and occurring in a quasi-crossing region between initial $K^+(3p^6)-Ar(3p^6)$ and charge transferred $K(4s) + Ar(3p^6)$ and/or $K(4p) + Ar(3p^6)$ terms of $\Sigma - \Sigma$ symmetry.

3. Na^+-He collisions

The same procedure, as for the K^+-Ar collision is applied to determine the mechanism for charge exchange processes occurring in Na^+-He collisions. Two sets of experimental results are obtained in our study: one by the refined version of the capacitor method for measuring the total charge exchange cross sections of the prosesses

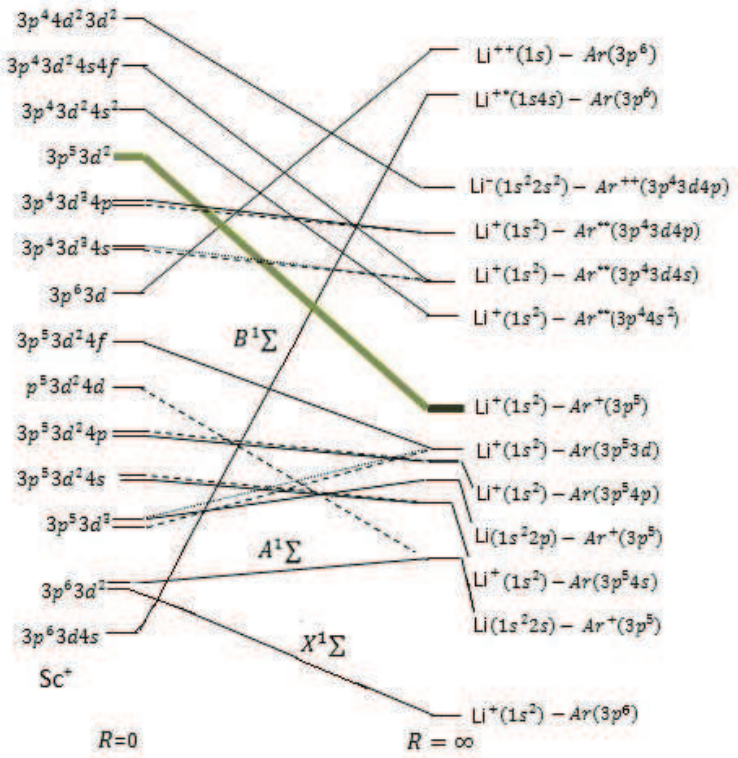

FIG. 5: Schematic correlation diagram for some states of the $Li^+ - Ar$ collision system. Solid lines indicate Σ states, dashed lines indicate Π states and dotted lines indicate Δ states.

$$\mathrm{Na}^+ + \mathrm{He} \rightarrow \mathrm{Na}(2p^6 3s) + \mathrm{He}^+(1s), \quad (9)$$
$$\rightarrow \mathrm{Na}(2p^6 3p) + \mathrm{He}^+(1s), \quad (10)$$
$$\rightarrow \mathrm{Na}(2p^6 3d) + \mathrm{He}^+(1s), \quad (11)$$

when the sodium atom is in various states shown by curve 3a and the second one by optical measurements for the excitation into the states of $\mathrm{Na}(2p^6 3p)+\mathrm{He}^+ + 21.5$ eV (curve 3c). The comparison of these results (curve 3a and curve 3c in Fig. 1) shows that the fraction of the total cross section related to the sodium excited atom via reaction (10) amounts roughly to 10% of the total cross section. Therefore, the charge-exchange processes in this study is mostly attributed to the reaction (9) with an electron capture to the ground state of the projectile. In Ref. [23] an estimate was performed, though for the fixed energy $E = 1.5$ keV, of the revealing contribution of various inelastic channels realized in the $Na^+ - He$ collisions to charge-exchange processes. The authors of Ref. [23] show that the direct one electron target excitation in the reaction $Na^+ - He^*(1s2s) + 20.6$ eV and charge exchange into the ground 3s state of $Na(3s) + He^+ + 19.44$ eV occur with high probabilities. The charge-exchange processes to the ground $3s$ state of sodium atom can occur, as one can see from the correlation diagram in Fig. 6, due to the direct pseudo-crossing of the term corresponding to the state $\mathrm{Na}(2p^6 3s)+\mathrm{He}^+(1s)$ with the initial state of the system $\mathrm{Na}^+(2p^6)+\mathrm{He}(1s^2)$. Since the $\mathrm{Na}^+(2p^6)+\mathrm{He}(1s^2)$ state has only Σ symmetry it follows that the $\Sigma - \Sigma$ transition play a dominant role in the charge-exchange processes.

B. Ionization in $Li^+ - Ar$, $K^+ - Ar$, and $Na^+ - He$ collisions

1. *$Li^+ - Ar$ collisions*

To discuss the mechanism responsible for the ionization in $Li^+ - Ar$ collisions, we construct a schematic correlation diagram shown in Fig. 5 according to the rules presented in Ref. [44], electron energy spectra obtained in our study

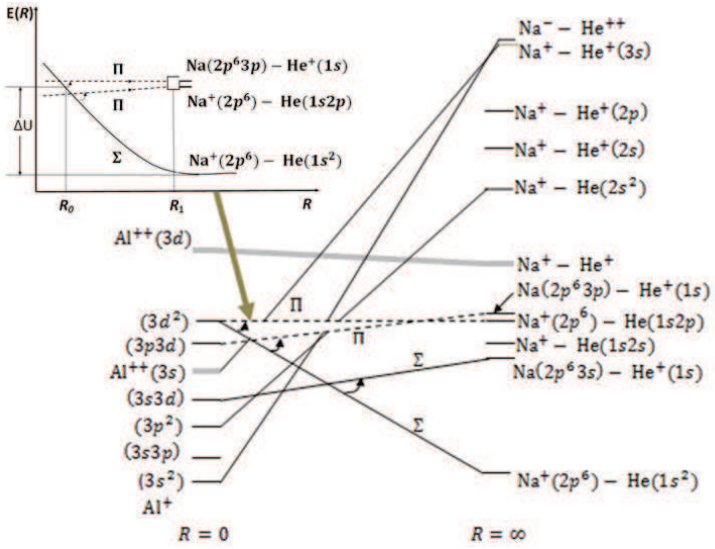

FIG. 6: Schematic correlation diagram for some states for the Na^+-He collision system. Solid lines indicate Σ states; dashed lines indicate Π states. The insert at the upper left corner shows the quasi-crossing of the ground state term of the system $Na^+(2p^6)-He(1s^2)$ with the $Na^+(2p^6)-He(1s2p)$ and $Na(2p^63p)-He^+(1s)$ terms. The arrow indicates the corresponding terms at the schematic correlation diagram at small internuclear distances..

and the data of differential cross section presented in Ref. [42]. This diagram is used for identification of the ionization mechanism. It follows from the results of the present measurements of the energy of the electrons ejected in Li^+-Ar collisions, that the liberation of mostly slow electrons with energies less than 10 eV is a characteristic of the ionization in Li^+-Ar collisions. In order to determine the mechanism responsible for this feature, we estimated the contribution of several inelastic processes which result in the emission of slow electrons to the total ionization cross section. In order to estimate the fraction coming from the autionization states of Ar atoms to the ionization cross section, the data for differential cross section obtained in Ref. [42] have been used. Integration of differential cross section shows, that the contribution of these processes to the total ionization cross sections amounts to just about 17%. Small contributions from atomic autoionization to the total ionization processes follow also from analyses of the correlation diagram in Fig. 5. As it is seen that none of the autoionization terms have an immediate crossing point with the system of ground states and hence, as one can expect, their population occurs with small probabilities.

To the best of our knowledge there are no experimental data in the literature which could be used to make estimates of other contributions to total ionization cross section. In order to estimate the contribution of direct ionization $Li^+(1s^2)+Ar(3p^6) \rightarrow Li^+(1s^2)+Ar^+(3p^5)+e$, which in the quasimolecular model is linked to the transition of an adiabatic term into the continuum, we use the procedure described in Ref. [40]. Analysis of the correlation diagram of the molecular orbital for the $(LiAr)^+$ system in Fig. 5 shows that in the united atom limit, the $3p$ state of the Ar atom evolves into the $3d$ state of the Sc^+ ion. Since this result is of importance for evaluation of the contribution of the direct ionization, we note that it agrees with the Barat-Lichten correlation rules [40], and the Eichler-Wille rules [45]. Consequently, the value $l = 2$ was chosen for the evaluation of the cross section. The binding energy E_{nl} of the electrons in the nonadiabatic region was chosen to be equal to that of the $3d$ electrons of the Sc^+ ion. The effective charge Z_{eff} was determined by the interpolation of the data from Ref. [43], and for the $3d$ electrons of the Sc^+ ion Z_{eff} =4.8. The estimate of the cross section for the direct ionization with these parameters are in reasonable agreement with our measurements (curves 2a and 2c in Fig. 2): the absolute value of the cross sections are closer and the energy dependences are similar.

The same procedure was used to estimate the contribution of stripping processes, that are also the source of electrons, to the ionization cross section. The correlation diagram in Fig. 5 indicates that the $1s$ state of the Li^+ ion correlates with the $3d$ state of the scandium ion Sc^+ in the united atom limit. The binding energy of these electrons is known [46] and hence future calculation become possible. Estimates of the contribution for the stripping processes with these parameters show, that at the ion energy of 3.0 keV the contribution of the stripping processes to the total ionization cross section is less than 0.4%, while at 6.0 keV it is less than 2%. Therefore, this contributions of the stripping processes are insignificant over the entire energy range studied.

Although the above mentioned agreement of the estimation for the direct ionization with the experiment is fortuitous to some extent, this result together with the estimate of portion for the atomic autoionization and the stripping allows us to conclude, that the contribution of direct ionization process to the total cross section for the electron emission is

the governing mechanism for the Li^+-Ar collisions.

2. K^+-Ar collisions

It follows from the results of the present measurements of the electron ejection cross sections that the liberation of electron with energies in the range $20 < E_e < 32$ eV strongly contribute to the ionization in K^+-Ar collisions. As the result for energy-loss spectrum for the K^+-Ar collision (see Fig. 4) among the different processes that lead to ionization of the target atom with above mentioned energy of electrons, a decisive role may be played by the processes of autoionization and of ionization with excitation of the Ar atom. From the energy-loss spectrum plotted in Fig. 4 it is seen that these processes are represented by the fourth peak of that spectrum. As it will be shown below, contribution of direct ionization (direct removal of an electron to the continuum spectrum with formation of an intermediate autoionization state) and multiple ionization of the target atom, make no noticeable contribution to the effective cross section for the target atom ionization. In order to determine the channel and mechanism of ionization we estimate the contribution of direct ionization $K^+(3p^6)+Ar(3p^6) \rightarrow K^+(3p^6)+Ar^+(3p^5) + e$ that in the quasimolecular model is linked to the transition of the adiabatic term to the continuum. We estimate the cross section of this process using the results obtained in Ref [40]. It should be noted that the expression given in Ref. [40] is written in terms of the principal quantum number for a hydrogen-like ion. Therefore, we modify it slightly for the estimation of the cross section for the emission of electrons from multi-electron atoms. The final expression which is used here can be found in our previous work [22]. We use this expression for the interpretation of the results for the Li^+-Ar and it will be employed for the Na^+-He collision systems in the next subsection.

An analysis of correlations for molecular orbitals in one-electron approximation for the K^+-Ar system shows that the $3p$ electrons of the Ar atom, whose ionization is considered, in the limit of the united atom correspond to the $4d$ electrons of Rb^+ ion. Thus, for the estimation we chose the orbital angular momentum $l = 2$. The binding energy E_{nl} of electrons, in the nonadiabaticity region, was assumed to be equal to the binding energy of $4d$ electrons of the Rb^+ ion. Since it would be difficult to determine accurately the effective charge Z_{eff} and binding energy E_{nl} for the $4d$ electrons of the Rb^+ ion, being in the excited states with the electron configuration of Ar like ion $[Ar]3d^64p^24f^24d^55f^2$, the effective charge Z_{eff} was determined by the interpolation of the results obtained by a Hartree method [43] in Ref. [42]. Estimates of the cross section for the direct ionization with these parameters show, that at an ion energy of $E = 2$ keV the contribution of the direct ionization to the total ionization cross section is less than 1.5%, while at $E = 7.0$ keV it is less than 2.5% and, hence, its average value does not exceed $3.5{\cdot}10^{-18}$ cm^2. This means that this contribution is insignificant over the entire energy range studied. According to these calculations and based on the results, obtained in our study for the energy of liberated electrons, we can conclude that the primary mechanism for the ionization is connected with the decay of autoionization states. As seen from the energy-loss spectrum for the K^+-Ar collision system (Fig. 4), indeed the states with energies of $25-34$ eV are excited with noticeable probability. These energies correspond to the autoionization states of Ar atom with excitation of one $3s$ electron and two $3p$ electrons with configurations of $3s3p^64s$ and $3p^4(^1D)4s(^2D)4p(^1P)$, respectively.

3. Na^+-He collisions

The liberation of electrons with the energies less than 17 eV is a characteristic of ionization processes in Na^+-He collisions as it follows from the results of present measurements of emitted electrons. In order to reveal the channels and establish the mechanism responsible for the ionization, we estimate the contribution of several inelastic processes that result in emission of slow electrons. Using the Barat – Lichten rules [44] and the data from Ref. [23] we construct the correlation diagram presented in Fig. 6. The contribution of the direct ionization $Na^+(2p^6) + He(1s^2) \rightarrow Na^+(2p^6) + He^+(1s) + e$ is estimated following Ref. [40]. An analysis of the correlation diagram of molecular orbitals for the Na^+-He system shows, that the $1s$ state of the He atom, whose ionization is considered, in the limit of the united atom becomes the $2p$ state of the Al^+ ion. Thus, for the estimate of cross section we chose the orbital angular momentum $l = 1$. The binding energy E_{nl} of the electrons in the nonadiabatic region was chosen to be equal to the $2p$ electrons of the Al^+ ion (28.75 eV). The effective charge Z_{eff} was determined by the interpolation of the data obtained by a Hartree calculation in Ref. [43]. For the $2p$ electrons of the Al^+ ion, we obtain $Z_{eff} = 3.7$. The estimate of the cross section for the direct ionization with these parameters shows, that at an ion energy of 1.5 keV the contribution of the direct ionization to the total ionization cross section is less than 5.5%, while at 6.5 keV it is less than 7%.

The same procedure is applied to determine the contribution of the electron yield to the measured ionization cross section as a result of stripping of the projectile ions. As it follows from the diagram in Fig. 6 the $2p$ state of the Na+ ion is correlated with the $3d$ state of the Al^+ ion. Consequently, for calculation of the cross section we select $l = 2$,

while we take Z_{eff} to be the same as for the $2p$ electrons of the Al^+ ion used in evaluating the ionization cross section. As a result of this calculation we find that the contribution of stripping to the total electron emission cross section is less than 12% for the energy of 1.5 keV of the sodium ions and does not exceed 17% for the energy of 6.5 keV. Consequently, we can conclude that the contribution of the stripping processes as well as direct ionization processes to the total ionization cross section is insignificant in the entire energy range interval studied. Other possible sources for liberation of the electrons like e.g. double ionization of the He atom, $Na^+ + He \rightarrow Na^+ + He^{2+} + 2e$, and direct two-particle excitation $Na^+ + He \rightarrow Na^{+^*}(2p^5 3s) + He^*(1s2s)$ and capture accompanied by the ionization of the He^+ ion that is also a possible source for electron liberation via reaction $Na^+ + He \rightarrow Na + He^{+^*} \rightarrow Na + He^{2+} + e$, evidently make a small contribution to the ionization cross section. There are two reasons for this. The absence of pseudo-crossings of the corresponding quasimolecular terms with the ground state term, as it seen from the diagram in Fig. 6, and the large energy defect for these processes, 54 eV, 53.9 eV and 48.9eV respectively. Consequently, by systematically evaluating the contribution of various inelastic processes to the ionization of the target atoms in $Na^+ - He$ collisions, we find that the ionization may be caused primarily by the decay of autoionization states in an isolated atom. This assessment is supported by the correlation diagram in Fig. 6 and by the data obtained in Ref. [23] as well. According to Ref. [23] these states are those with two excited electrons associated with a direct two electron excitation of the He atom in autoionization state: $Na^+ + He \rightarrow Na^+ + He^{**}(2s^2) \rightarrow Na^+ + He^+ + e$.

C. Excitation processes in $K^+ - Ar$ and $Na^+ - He$ collisions

1. $K^+ - Ar$ collisions

In discussing the mechanism for the $Ar(3p^5 4s)$ excitation processes in $K^+ - Ar$ collisions we use the energy-loss spectrum obtained in our study and results reported in Ref. [7]. In Ref. [7] the area corresponding to the energy-loss range of $11.5 - 16$ eV has been integrated and for the sum of Ar excited states $3p^5 4s$, $3p^5 4p$ and $3p^5 3d$ we obtained a value of $7 \cdot 10^{-17}$ cm^2. Since the above mentioned excited levels are energetically close as seen in Fig. 4, the determination of the relative probabilities of their excitation encounters considerable difficulties. Moreover, as shown by a qualitative analysis of the energy-loss spectrum (the shape of the peak and the position of its maximum), the levels for the configurations of $3p^5 4p$ and $3p^5 3d$ are excited with high probability, while the level for the configuration $3p^5 4s$ is populated with a surprisingly small probability although the level of $3p^5 4s$ state lays at lower energy than the levels $3p^5 4p$ and $3p^5 3d$, ($11.5 - 12$ eV and $13 - 14$ eV respectively, see Fig. 4). This fact and also the requirement to have reliable data related to the individual channel, that includes the clarification of the contribution of various excitation processes and determination of mechanisms for the processes, motivate us to perform optical measurements for the resonance $Ar(3p^5 4s)$ line in the reaction (7).

The analysis of the spectrum for the $K^+ - Ar$ collision system presented in Fig. 4 shows that the second peak in the energy-loss spectrum with the width of $11.5 - 16$ eV corresponds not only to the excitation processes, but also to the direct ionization of the Ar atom (the ionization potential 15.7 eV). Our estimate shows that, the value of direct ionization cross section for the $K^+ - Ar$ collision system amounts to a magnitude of $2.8 \cdot 10^{-18}$ cm^2. As seen from our results given by curve 1a in Fig. 3 the average excitation cross section for the resonance Ar line in the $3p^5 4s$ state amounts to $1 \cdot 10^{-17}$ cm^2. Thus, due to the smallness of the direct ionization cross section as well as the excitation cross section for the resonance $Ar(3p^5 4s)$ line, compared to the sum of the excitation cross sections $7 \cdot 10^{-17}$ cm^2, one can conclude that the dominant role in the Ar excitation processes is played by the excitation of the $3p^5 4p$ and $3p^5 3d$ states. As for the mechanism for the excitation of resonance $3p^5 4s$ state of the Ar atom, its population is caused by a cascade transition from already mentioned upper laying levels $3p^5 4p$ and $3p^5 3d$ to the resonance $4s$ level.

2. $Na^+ - He$ collisions

The oscillatory structure of the energy dependence of the cross sections is most pronounced for the $Na^+ - He$ collision system. Our results show that the oscillation on the excitation cross sections for the resonance lines of sodium and helium (curve 3a and curve 2a in Fig. 3) atoms are in antiphase. The curve obtained by adding of the excitation cross sections of these lines turns out to be smooth over the entire energy range (curve 4a in Fig. 3). This means that the observed oscillations are a consequence of interference of two energetically neighboring vacant excited states (the difference between the states is 0.03 eV) of the systems $Na^+(2p^6) + He(1s2p)$ and $Na(2p^6 3p) + He^+(1s)$ interacting at large internuclear distance.

On the other hand, for the realization of a quasi-molecular interference phenomenon it is necessary that both of these excited terms to be populated by the same entrance term. As seen from the correlation diagram in Fig. 6 this term may correspond to the ground state $Na^+(2p^6) + He(1s^2)$, which in the limit of united atom promotes to

the autoionization state of aluminum ion $Al^+(3d^2)$. Therefore, the ground state term, which possess Σ symmetry, populates Π terms of the $Na(2p^6 3p)$ + $He^+(1s)$ and $Na^+(2p^6)$ +$He(1s2p)$ states at small internuclear distance due to the rotational $\Sigma - \Pi$ transition and then at a large R an interaction of the terms with the same $\Pi - \Pi$ symmetry take place.

The experimental results for the excitation function for the resonance lines of sodium and helium atoms, as well as the mechanisms defined for these processes, allows us to obtain additional information regarding the restoration of parameters for the interaction area. For this reason we use the procedure suggested in Ref. [47]. The insert in Fig. 6 shows the quasi-crossing of the ground state term of the system $Na^+(2p^6)$−$He(1s^2)$ with the $Na^+(2p^6)$−$He(1s2p)$ and $Na(2p^6 3p)$−$He^+(1s)$ terms at small internuclear distances. Taking into consideration that a quasi-crossing of ground state term and the later excitation terms that are populated at small internuclear distance [48], the experimental data allow to determine the mean value of threshold energy ΔU for the excited states at the average internuclear distance R_0 and the area of "rectangular loop" formed by the terms of these states, shown in the insert in Fig. 6. The area of "rectangular loop", which consists of the terms of these states, is $\langle \Delta E \cdot R \rangle$, where ΔE is the splitting energy of the terms and R is the internuclear distance. The estimate shows that ΔU =70 eV and the value of $\langle \Delta E \cdot R \rangle \sim 1.4 \cdot 10^{-7}$ eV·cm. The value of ΔU corresponds to the excitation energy at the quasi-crossing of the ground state term and terms of interference states. Using a potential energy curve for the ground state of the system $(NaHe)^+$ from Ref. [49] and the value ΔU =70 eV determined from our data, one can unambiguously obtain that the quasi-crossing of the terms occurs at $R \sim 0.5$ $\mathring{A}$ internuclear distance.

It is well established that for a small internuclear distance $\Sigma - \Pi$ transitions, which are related to a rotation of the internuclear axis, are the most important. Under such condition, the absolute value of the cross section should be small and by increasing the velocity of relative motion of particles it should increase, reaching maxima at comparatively large velocities. Our data confirm this assumption. Moreover, comparatively large oscillation depth, observed in our study, and the data reported in Ref. [50] support the assumption that at large internuclear distances the interaction of the terms with the same $\Pi - \Pi$ symmetry take place, which itself are populated due to the rotational transition.

V. SUMMARY AND CONCLUSIONS

In this study we report the measurements for absolute differential and total cross sections for charge-exchange, ionization and excitation processes in Li^+−Ar, K^+−Ar, and Na^+−He collisions in the energy range of 0.5−10 keV. We have also measured the energies of the electrons liberated in the collisions and found that the energy of most of the liberated electrons are below 12 eV for the Li^+−Ar collision, within the interval $20 - 32$ eV for the K^+−Ar collision system, and less than 17 eV for the Na^+−He collision. The measurements are performed under the same experimental conditions, using a refined version of the condenser plate method, the collision spectroscopy method with angle- and energy-dependent detection of the collision products, and the optical spectroscopy method, with an accurate calibration procedure of the light recording system. The comparison of our measusrements with existing experimental and theoretical results are presented.

We construct the correlation diagrams for the $(LiAr)^+$ and $(NaHe)^+$ systems based on the rules formulated in Ref. [44]. The experimental data and the schematic correlation diagrams are used to analyze and determine the mechanisms for the charge-exchange, ionization and excitation processes for the reactions (1)-(8). We found that the charge-exchange processes occur with high probabilities and electrons predominately are captured to the ground states of the resultant atom in the region of pseudocrossing of potential curves of Σ symmetry. The contribution to the charge-exchange cross section for the Li^+−Ar collision from the transition corresponding to $R \sim 1.5$ a.u. is the dominant one. The results of experimental studies show that the cross sections ratio for charge-exchange, ionization and excitation processes roughly attains the value $10 : 2 : 1$, respectively. The contributions of various partial inelastic channels to the total ionization cross section are estimated and primary mechanism for this process is defined. The contribution of the direct ionization process to the total cross section for the electron emission is the governing mechanism for the Li^+−Ar collision. The primary mechanism for the ionization in the K^+−Ar collision is connected with the decay of autoionization state. Our results confirm the conclusion of Ref. [23] that the ionozation in the Na^+−He collision is related to a direct two electron excitation of the He atom in autoionization state: $Na^+ + He \rightarrow Na^+ + He^{**}(2s^2) \rightarrow Na^+ + He^+ + e$.

The energy-loss spectrum is applied to estimate the relative contribution of different inelastic channels and to determine the mechanisms for the ionization and for some excitation processes. The main mechanism for the excitation of resonance $3p^5 4s$ state of the Ar atom in the K^+−Ar collision is related to the cascade transition from upper laying levels $3p^5 4p$ and $3p^5 3d$ to the resonance $4s$ level. The oscillatory structure of the energy dependence of the cross sections is most pronounced for the Na^+−He collision system. This behavior is observed in the excitation function for the helium resonance line ($\lambda = 58.4$ nm, $2p - 1s$ transition) and for the sodium doublet lines $\lambda = 589.0$ nm and

$\lambda = 589.6$ nm, $3p - 3s$ transition in $Na^+ -$ He collisions. We conclude that this phenomenon is a consequence of interference of two energetically separated by 0.03 eV excited states of the $Na^+(2p^6)$ + $He(1s^2)$ $\rightarrow$Na$(3p)$+ $He^+(1s)$ and $Na^+(2p^6)$+$He(1s^2)$ $\rightarrow$$Na^+(3p^6)$+ $He(1s2p)$ systems at large internuclear distances.

Acknowledgements

This work was supported by the Georgian National Science Foundation under the Grant No.31/29 (Reference No. Fr/219/6-195/12). R.Ya.K. and R.A.L gratefully acknowledge support from the International Reserch Travel Award Program of the American Physical Society, USA.

[1] I. P. Flaks, B. I. Kikiani, and G. N. Ogurtsov, Tech. Phys. **10**, 1590 (1966).
[2] G. N. Ogurtsov and B. I. Kikiani, Tech. Phys. **11**, 362 (1966).
[3] J. P. Mouzon, Phys. Rev. **41**, 605 (1932).
[4] D. E. Moe and O. H. Petsch, Phys. Rev. **110**, 1358 (1958).
[5] V. B. Matveev, S. V. Babashev, and V. M. Dukelski, Sov. Phys. JETP **28**, 404 (1969).
[6] V. B. Matveev and S. V. Babashev, Sov. Phys. JETP **30**, 829 (1970).
[7] V. V. Afrosimov, S. V. Bobashev, Yu.S. Gordeev, and V. M. Lavrov, Sov. Phys. JETP **35**, 34 (1972).
[8] R. Francois, D. Dhuicq, and M. Barat, J. Phys. B: At. Mol. Phys. **5,** 963 (1972).
[9] D. C. Lorents and G. M. Conklin J. Phys. B: At. Mol. Phys. **5,** 950 (1972).
[10] Z. Z. Latypov, A.A. Shaporenko, Sov. Physics JETP, **42**, 986 (1976).
[11] S. Kita, K. Noda, and H. Inouye, J. Chem. Phys. **63**, 4930 (1975).
[12] V. V. Afrosimov , Yu .S. Gordeev, and V. M. Lavrov Sov. Phys. JETP **41**, 860 (1976).
[13] Yu. F. Bidin and S. S. Godakov, Sov. Phys. JETP Lett. **23**, 518 (1976).
[14] 14. R. A. Lomsadze, M. R. Gochitashvili, Phys. Rev. A **92**, 062703 (2015).
[15] K. Jrgensen, N. Andersen, and J. Olsen, J. Phys. B **11**, 3951 (1978).
[16] J. O. Olsen, T. Andersen, M. Barat et al., Phys. Rev. A **19**, 1457 (1979).
[17] S. Kita, T. Hasegawa, H. Tanuma, and N. Shimakura, Phys. Rev. A **52**, 2070 (1995).
[18] S. Kita, S. Gotoh, N. Shimakura, and S. Koseki, Phys. Rev. 62, 032704 (2000).
[19] R. A. Lomsadze, M. R. Gochitashvili, R. V. Kvizhinadze, N. O. Mosulishvili, and S. V. Bobashev, Tech. Phys. **52**, 1506 (2007).
[20] S. Kita, S. Gotoh, T. Tanaka et al., J. Phys. Soc. Jpn. **76**, 044301 (2007).
[21] S. Kita, T. Hatada, and H. Inoue, Y. Shiraishi, and N. Shimakura J. Phys. Soc. Jpn. **82**, 124301 (2013).
[22] R. A. Lomsadze, M. R. Gochitashvili, R. Ya. Kezerashvili, N. O. Mosulishvili, and R. Phaneuf, Phys. Rev. A **87**, 042710 (2013).
[23] S. Kita, T. Hattori, and N. Shimakura, J. Phys. Soc. Jpn **84**, 014301 (2015).
[24] B. R. Junker and J C Browne, Phys. Rev. A **10,** 2078 (1974).
[25] V. Sidis, N. Stolterfoht, and M. Barat, J. Phys. B: At. Mol. Phys. **10,** 2815 (1977).
[26] S.V. Bobashov Phys.Lett. A. **31**, 204 (1970).
[27] R. Odom, J. Caddick, and J. Weiner, Phys. Rev. A **15**, 1414 (1977).
[28] S.V. Bobashev, V.A. Fritskii, J. Exp. and Theor. Phys. Lett., **12**, (1970).
[29] B. I. Kikiani, R. A. Lomsadze, and N. O. Mosulishvili et al., Tech. Phys. **30**, 934 (1985).
[30] M. R. Gochitashvili, R. A. Lomsadze et al., Georgian Electron. Sci. J.: Phys. **39**-2, (2004).
[31] M. R. Gochitashvili, N. Jaliashvili, R. V. Kvizhinadze, and B. I. Kikiani, J. Phys. B **28**, 2453 (1995).
[32] R. A. Lomsadze, M. R. Gochitashvili, R. Ya. Kezerashvili, Phys. Rev. A **82**, 022702 (2010).
[33] J. M. Ajello and B. Franklin, J. Chem. Phys. **82**, 2519 (1985).
[34] S. V. Avakyan, R.N. Ii'In, V.M. Lavrov, G.N. Ogurtsov, Collision processes and excitation of UV emission from planetary atmospheric gases: a handbook of cross sections, 1999 - books.google.com
[35] E. J. Stone and E. C. Zipf, J. Chem. Phys. **56**, 4646 (1972).
[36] K. H. Tan and J. W. McConkey, Phys. Rev. A **10**, 1212 (1974).
[37] W.R. Pendelton and R.R. O'Niel, J. Chem. Phys. **56**, 62601 (1972).
[38] B.N.Srivastava and I.N.Mirza, Phys. Rev.168, 86 (1968).
[39] S. Kita M. Izawa, and H.Inouye, J. Phys.B: At. Mol. Phys. **16** L499 (1999).
[40] E. A. Solov'ev, Sov. Phys., JETP **54**, 893 (1981).
[41] W. Maurer and K. Mehnert, Z. Phys. **106**, 453 (1937).
[42] M. Barat, D.Dhuieq, R.Francois and V. Sidis, J.Phys. B: Atom. Molec. Phys., **6**, 2072 (1973).
[43] R. D. Hartree, The Calculation of Atomic Strictures, Wiley, New York, 1957.
[44] M. Barat and W. Lichten, Phys. Rev. A **6**, 211 (1972).
[45] J. Eichler. U. Wille, B. Fastrup, and K. Taulbjerg, Phys. Rev. A 14, 707 (1976).

[46] J.A. Bearden, A.F. Burr, Rev. Mod. Phys. **39**, 125 (1967).
[47] N.H. Tolk, C.W. White, S.H. Neff, and N. Lichten, Phys. Rev. Lett., **31**, 671 (1973).
[48] S.V. Bobashev, Advances in atomic and molecular physics, **14**, 341 (1978).
[49] V.K. Nikulin and Yu.N. Tsarev, Chem. Phys., **10**, 433 (1975).
[50] S.V. Bobashev and V.A. Kharchenko, Sov. Phys. JTEF, **44**, [Zh. Eksp.Teor. Fiz. **71**, 1327 (1976).